

Electronic Supplementary Information

Electro-active Phase Formation in PVDF-BiVO₄ Flexible Nanocomposite Films for High Energy Density Storage Application

Subrata Sarkar, Samiran Garain, Dipankar Mandal* and K. K. Chattopadhyay*

Department of Physics, Jadavpur University

Kolkata 700 032, India

E-mail address:

dipankar@phys.jdvu.ac.in (D. Mandal)

kalyan_chattopadhyay@yahoo.com (K. K. Chattopadhyay)

Determination of direct & indirect band gap energies from UV-Vis data

The band gap energies (E_g) of the BiVO_4 -NPs were determined from the $(\alpha h\nu)^{1/n}$ versus wavelength traces. The fundamental absorption, which corresponds to electron excitation from the valence band to the conduction band, can be used to determine the nature and value of the optical band gaps. The relation between the absorption coefficient (α) and the incident photon energy ($h\nu$) can be written as $(\alpha h\nu)^{1/n} = A(h\nu - E_g)$

where A is a constant, E_g is the band gap energy of the material, and the exponent n depends on the type of the transition. The values of n for direct allowed, indirect allowed and direct forbidden transitions are $n= 1/2, 2,$ and $3/2,$ respectively. To determine the possible transitions, $(\alpha h\nu)^{1/n}$ data versus $h\nu$ were plotted, and the corresponding band gaps were obtained by extrapolating the steepest portion of the graph on the $h\nu$ axis at $(\alpha h\nu)^{1/n} = 0$. Fig. S1 shows the $(\alpha h\nu)^2$ versus $h\nu$ plots to determine the direct band gap energy, while Fig. S2 shows the $(\alpha h\nu)^{1/2}$ versus $h\nu$ plot to determine the indirect band gap energy. The direct and indirect band gap energies of the BiVO_4 -NPs were found to be 4.14 and 3.64 eV, respectively.

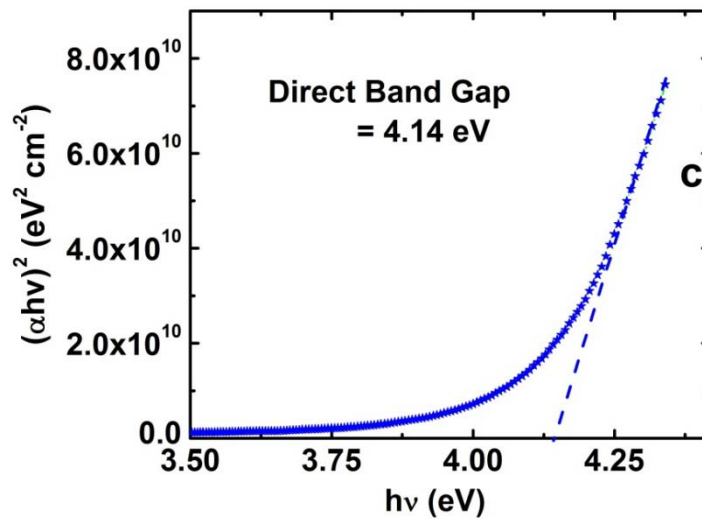


Fig. S1. Plot for determination of the direct band gap energy of the BiVO_4 -NPs from UV-Vis spectra.

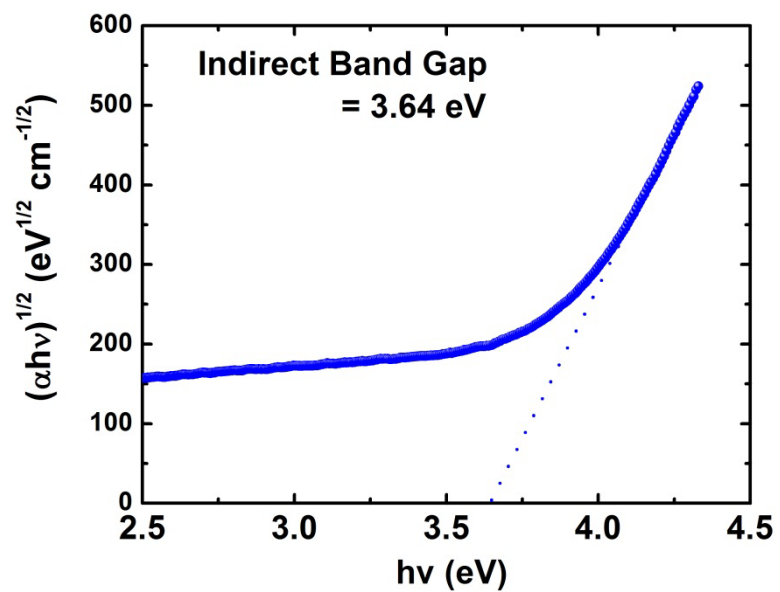


Fig. S2. Plot for determination of the indirect band gap energy of the BiVO₄-NPs from UV-Vis spectra.

Calculation of Crystallinity (X_c) from the XRD analysis

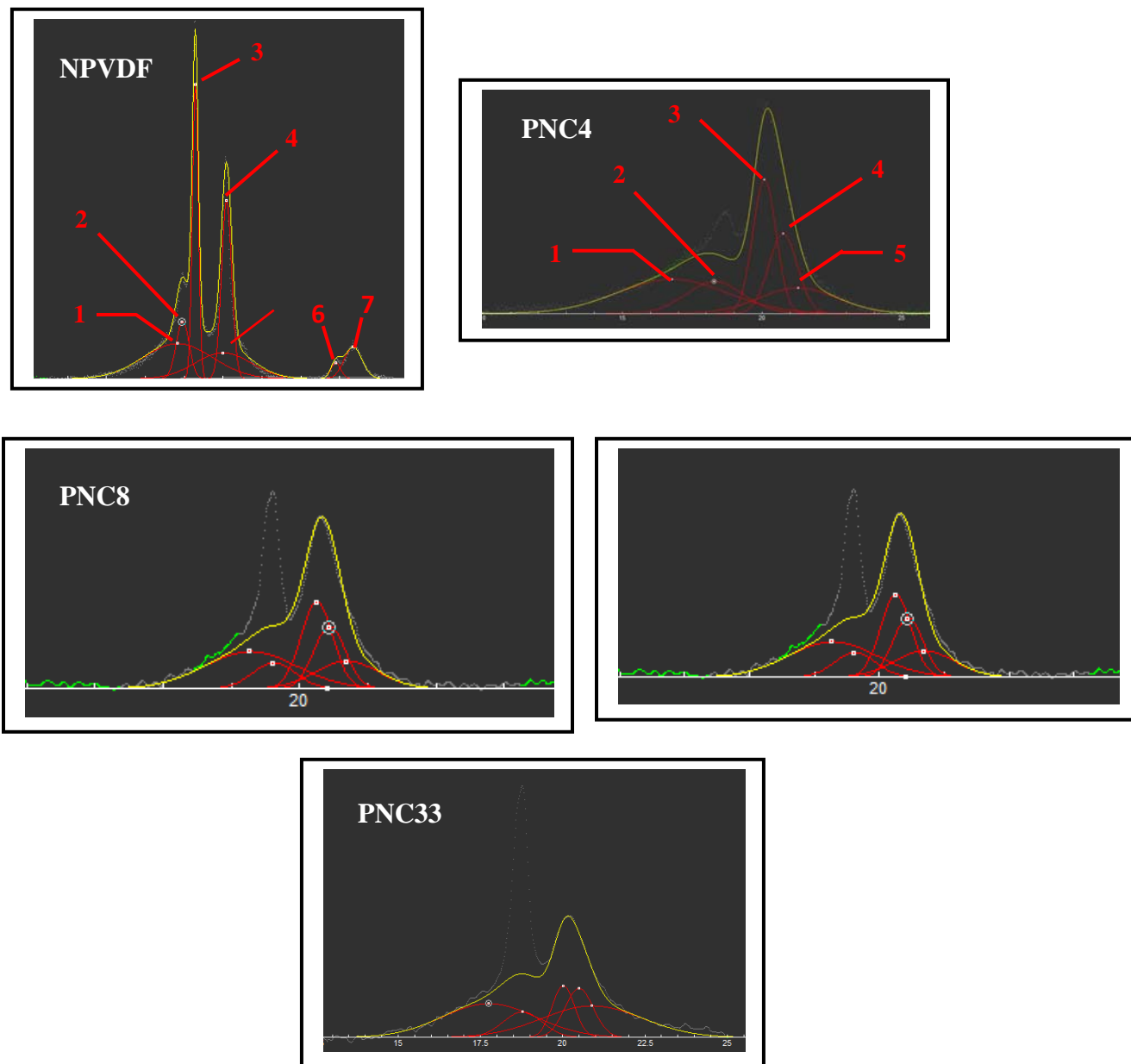


Fig. S3. The curve deconvolution of XRD pattern of neat PVDF (NPVDF) and PNC films

In NPVDF, the broad (1 and 5) halos are due to the amorphous contributions and others peaks (*i.e.*, 2, 3, 4, 6 and 7) are the characteristic peaks (α -phase) of the crystalline counterpart.

In the polymer nanocomposite films (PNC4, PNC8, PNC16 and PNC33), 1 and 5 broad halos indicates the amorphous regions and other peaks (2 to 4) are the due to crystalline contributions arising from the

polymer matrix. The crystalline peaks (for example, in the figure, at $2\theta=18.6$) from BiVO_4 NPs are exempted in calculation of crystallinity in the PNC films. The ratio of the crystalline and amorphous content and % of crystallinity are listed in table S1.

Table - S1. The ratio of the crystalline and amorphous content and % of crystallinity of neat PVDF and polymer nanocomposites.

Samples	$\frac{\sum A_{cr}}{\sum A_{amr}}$	$X_c = \frac{\sum A_{cr} / \sum A_{amr}}{1 + \sum A_{cr} / \sum A_{amr}} \times 100 \%$
NPVDF	1.29	56.3 %
PNC4	1.26	55.8 %
PNC8	0.92	48.0 %
PNC16	0.90	47.4 %
PNC33	0.67	40.1 %

$\frac{\sum A_{cr}}{\sum A_{amr}}$ indicates the ratio between the total area of crystalline peaks and total are of the amorphous halo. X_c is the % of crystallinity attributed to the PVDF.

Table - S2

Samples	Crystallization Temperature ($^{\circ}\text{C}$)	Crystallinity content X_C (%)	
	t_{XC}	DSC	XRD
NPVDF	135.6	55.4	56.3
PNC4	137.8	55.2	55.8
PNC8	140.1	52.3	48.0
PNC16	142.4	52.0	47.4
PNC33	143.6	48.2	40.1

t_{XC} : Crystallization temperature; X_C : Crystallinity content.

Optical Polarizing Microscopic Study

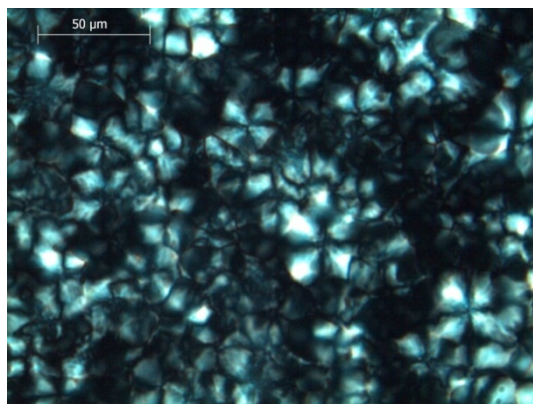


Fig. S4. Cross polarized optical microscopy (CPOM) image of NPVDF film.

Fig.S4 shows the CPOM image of pure PVDF film, average spherulite diameter $\approx 40\mu\text{m}$, while only dark CPOM images were obtained for the PNC4, PNC8, PNC16 and PNC33 films which apparently means that there was no α - or γ -phase in the composite films but the XRD, FTIR and DSC studies on the same films shows β - and γ -phases. In these cases, we infer that the loading of BiVO_4 nanoparticle hinders the optical ray to appear to the microscope resulting in the dark CPOM images.

XPS Analysis

Table S3. The % change of area between PNC[†] and NPVDF, calculated from peak deconvolution of high resolution C1s and F1s XPS spectra^{††}.

Change of area (%)			
Δ_{ACF_2}	Δ_{ACH_2}	$\Delta\left(\frac{ACH_2}{ACF_2}\right)$	Δ_{AF1s}
5.5	3.8	9.0	5.0

[†]Here PNC8 sample was chosen for representation of all PNC samples.

^{††} Calculation

% change of CF₂ peak area when intensity is normalized to the CH₂ peak, *i.e.*,

$$\Delta_{ACF_2} = \frac{(ACF_2)_{NPVDF} - (ACF_2)_{PNC}}{(ACF_2)_{NPVDF}} \times 100 \% = 5.5\%$$

% change of CH₂ peak area when intensity is normalized at CH₂ peak, *i.e.*,

$$\Delta_{ACH_2} = \frac{(ACH_2)_{PNC} - (ACH_2)_{NPVDF}}{(ACH_2)_{NPVDF}} \times 100 \% = 3.8 \%$$

% change of ratio between area of CH₂ and CF₂ peaks, *i.e.*,

$$\Delta\left(\frac{ACH_2}{ACF_2}\right) = \frac{\left(\frac{ACH_2}{ACF_2}\right)_{PNC} - \left(\frac{ACH_2}{ACF_2}\right)_{NPVDF}}{\left(\frac{ACH_2}{ACF_2}\right)_{NPVDF}} \times 100 \% = 9.0 \%$$

% change of F1s peak area, *i.e.*,

$$\Delta_{AF1s} = \frac{(AF1s)_{PNC} - (AF1s)_{NPVDF}}{(AF1s)_{NPVDF}} \times 100 \% = 5.0\%$$

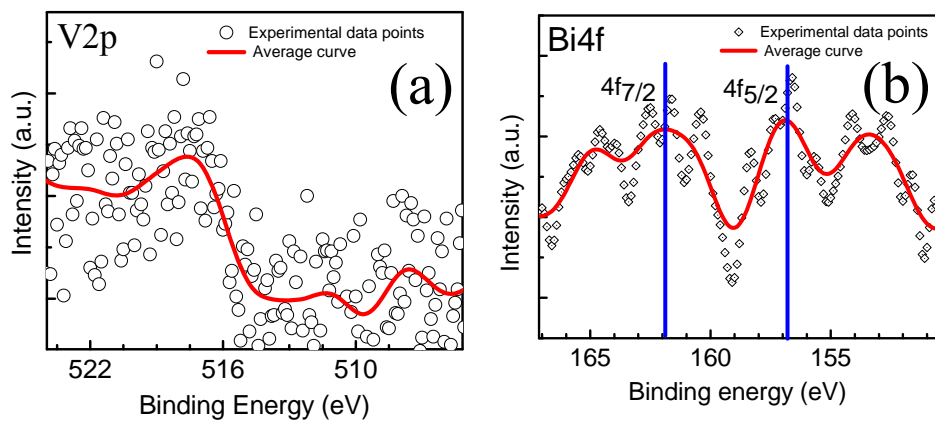


Fig. S5. The high resolution (a) V2p and (b) Bi4f core level XPS spectra of the PNC8 film.

Dielectric Data

The PNC films of our present work exhibit quite superior dielectric properties compared to literature values (tabulated in Table S4).

Table S4[†]

Dielectric		Filler in PVDF composite
Constant (ϵ_r)	Loss ($\tan\delta$)	
44	0.02	8 wt % BiVO ₄ -NPs ^{††}
17	0.02	10 wt% PVDF-graphite ²⁶
38	0.13	50 vol. % of BT ⁴
14.7	0.02	10 vol. % BT/SiO ₂ ⁶
58	1.5	11 wt % MgO ²⁷
37	0.5	30 vol.% of c-BT ⁷
21	0.07	BT-SAND ⁸
11	0.07	7 wt% Graphite NS ²⁸
21	0.7	Silver-NPs ⁹
27	×	TiO ₂ -NPs ¹⁰

[†] The table is based on the recent progress of the dielectric properties of PVDF nanocomposites where the dielectric loss is comparable with the present work. ^{††}: Present work; BT: BaTiO₃; c-BT: crude BaTiO₃; BT-SAND: BaTiO₃-Sandwich; NS: Nanosheet ; × : Data not available

AC conductivity

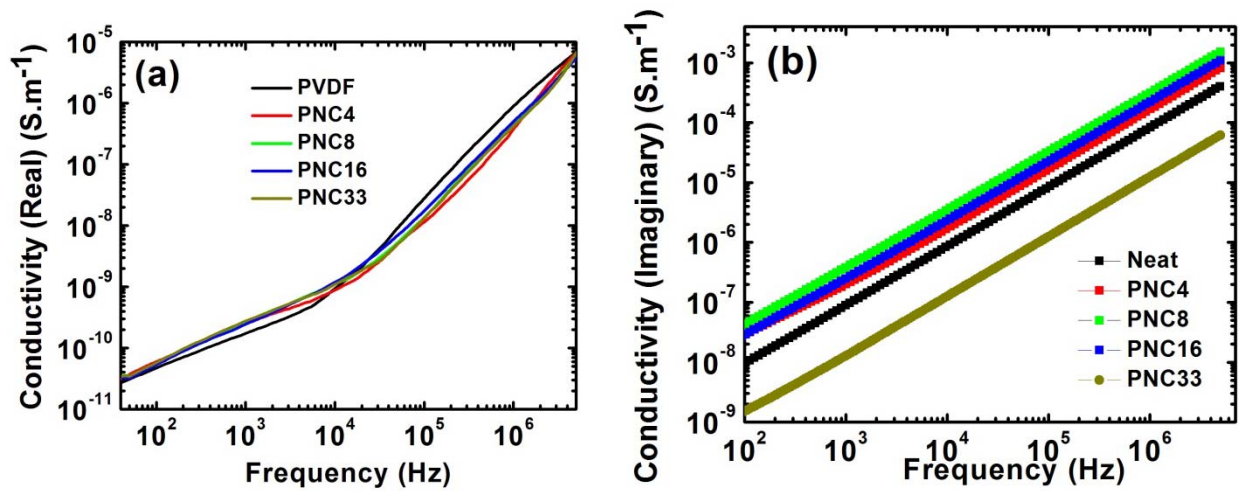


Fig. S6. Variation of real (a) and imaginary (b) part of ac conductivity with frequency.